SOLUTION OF THREE DIMENSIONAL EDDY CURRENT PROBLEMS BY INTEGRAL AND DIFFERENTIAL METHODS

R. Albanese and G. Rubinacci
Istituto di Ingegneria Elettronica - Universita' di Salerno
84100 Salerno - Italy

Abstract
A differential $\underline{T}$, Ω formulation using non conformal elements is presented. The results obtained with this formulation for different treatments of the boundary conditions at infinity are shown and compared among themselves and with respect to a $\underline{T}$ integral formulation.

INTRODUCTION

The determination of the eddy currents induced in the conductors by a time varying applied magnetic field is based on the solution of the quasi-stationary Maxwell's equations.

Several numerical methods have been proposed to overcome the well known difficulties related to this kind of open boundary problem.

In this paper we briefly summarize the main features of a number of methods based on integral and differential formulations [1,2,3], presenting a new differential $\underline{T}$, Ω approach which is the natural extension of the $\underline{T}$ integral formulation described in [3].

Eventually we exhibit some results obtained by applying the foregoing methods, in order to compare their efficiency in terms of storage occupation, CPU time and accuracy.

INTEGRAL FORMULATION

As far as linear non-magnetic media are concerned, it seems convenient to employ an integral formulation in terms of the current density vector $\underline{J}$:

$$\underline{J} \in S \tag{1.1}$$

$$\int_{V_c} \underline{w} \cdot (\underline{\underline{\eta}} \cdot \underline{J} + \frac{\mu_o}{4\pi} \int_{V_c} \frac{\dot{\underline{J}}'}{|\underline{x}-\underline{x}'|} d\tau' + \dot{\underline{A}}_e) d\tau = 0, \forall \underline{w} \in S \tag{1.2}$$

where V_c is the conducting region, $\underline{J}$ is the current density, $\underline{A}_e$ is the magnetic vector potential due to the external sources, $\underline{\underline{\eta}}$ is the resistivity tensor, and S is the set of the vector fields $\underline{s}$ verifying the following properties:

$$\underline{s} \cdot \hat{n} = 0 \qquad \text{on } \partial V_c \tag{2.1}$$

$$\oint_{\Sigma} \underline{s} \cdot \hat{n} \, d\Sigma = 0 , \qquad \forall \Sigma \text{ in } V_c \tag{2.2}$$

In order to fulfill Eq. (2.2), a current density vector potential $\underline{T}$ is introduced so as:

$$\underline{J} = \text{rot } \underline{T} \tag{3}$$

Having chosen shape and test functions for $\underline{T}$ according to the guidelines briefly summarized below, the following linear system results:

$$[L] [\dot{I}] + [R] [I] = [V] \tag{4}$$

where

$$\underline{J} = \sum I_k \underline{J}_k , \qquad \underline{w}_i = \underline{J}_i = \text{curl } \underline{T}_i \tag{5}$$

$$L_{ik} = \frac{\mu_o}{4\pi} \int_{V_c}\int_{V_c} \frac{\underline{J}_i \cdot \underline{J}'_k}{|\underline{x}-\underline{x}'|} d\tau d\tau' , \quad R_{ik} = \int_{V_c} \underline{J}_i \cdot \underline{\underline{\eta}} \cdot \underline{J}_k \, d\tau \tag{6}$$

$$V_i = - \int_{V_c} \dot{\underline{A}}_e \cdot \underline{J}_i \, d\tau \tag{7}$$

Eq. (3) does not yield a unique determination of $\underline{T}$, since the addition of the gradient of any scalar function does not modify its curl. This arbitrariness is removed by imposing a gauge for $\underline{T}$. The problem has been discussed in [2,5,6], where the constraint

$$\underline{T} \cdot \hat{u} = 0 \tag{8}$$

with $\hat{u}$ arbitrary direction, is shown to be the most efficient choice from the numerical point of view.

Applying this gauge, we have developed a finite element formulation described in detail in [3]. Here we recall only the main points of the method.

The degrees of freedom of the elements are associated to the path integrals ("tensions") of $\underline{T}$ along their edges [7,8]. In this case the set of independent tensions of $\underline{T}$ (the unknowns of the problem) is given by the branches of a co-tree associated to a fictitious network, made by the set of nodes and edges of the grid. Condition (2.1) is easily verified for simply connected regions if the tree is formed connecting firstly all the boundary nodes with boundary edges, and excluding from the set of the active edges also the branches of the co-tree which lie on the boundary. For the treatment of multiply connected regions and further details we refer again to [3].

DIFFERENTIAL FORMULATION

Several differential formulations have been already analyzed in literature. Among them we recall the $\underline{H}, \phi$ formulation proposed by Bossavit and Vérite [1], and the $\underline{T}$, Ω formulation discussed by Carpenter [5] and later by Brown [2].

Here we briefly remind the main points of the $\underline{T}$, Ω formulation and present a differential approach based on the same gauge used in our integral method [3].

The following weak formulation is employed:

$$\int_{V_c} \{\text{curl}\underline{T}_k \cdot \underline{\underline{\eta}} \cdot \text{curl}\underline{T} + \underline{T}_k \cdot \underline{\underline{\mu}} \cdot (\dot{\underline{T}} - \text{grad } \dot{\Omega})\} d\tau = 0, \ \forall \underline{T}_k \tag{9}$$

$$\int_R \text{grad } \Omega_k \cdot \underline{\underline{\mu}} \cdot (\underline{T} - \text{grad}\Omega) \, d\tau = 0, \ \forall \Omega_k \tag{10}$$

where $\underline{T} = \sum I_k \underline{T}_k + \underline{T}_s$, $\underline{T}_s$ is the vector potential associated with a prescribed current density distribution $\underline{J}_s$, $\underline{T}_k$ is the k-th shape function for $\underline{T}$ defined as before, Ω_k is the (standard isoparametric) k-th shape function for Ω, $\underline{\underline{\mu}}$ and $\underline{\underline{\eta}}$ are the magnetic permeability and electrical resistivity tensors, and V_c is the conducting region.

We remark that:

- the assumed shape functions for $\underline{T}$ and Ω are perfectly fitting when used together, as pointed out in [1,8];
- the dynamic matrix, resulting from a finite difference scheme in time, can be easily reduced to a banded symmetric one;
- the number of unknowns is exactly the same as in the H,ϕ formulation, as results from a simple analysis on the fictitious tree of the mesh.

One of the main advantages of a code based on this formulation is that it does not need a preprocessor to compute initial conditions and forcing fields due to given currents. Vector potential $\underline{T}_s$ and magnetic field $\underline{H}_s = \underline{T}_s - \text{grad } \Omega_s$ associated with the prescribed current density $\underline{J}_s$ can be readily computed by solving the following reducible system of equations:

$$\int_{V_c} \text{curl } \underline{T}_k \cdot (\text{curl}\underline{T}_s - \underline{J}_s) d\tau = 0, \ \forall \underline{T}_k \tag{11}$$

$$\int_R \text{grad } \Omega_k \cdot \underline{\underline{\mu}} \cdot (\underline{T}_s - \text{grad } \Omega_s) d\tau = 0, \ \forall \Omega_k \tag{12}$$

which are a particularization of the system (9),(10) to the magnetostatic case.

Furthermore, unlike the previous $\underline{T}$, Ω approaches, the current density vector potential is localized only inside the conducting region. This is made possible by the proper choice of the shape functions, which allow both magnetic field and current vector potential to have jumps in normal components across discontinuity

The $\underline{T}$, Ω formulation, like the other differential approaches, has to cope with the treatment of boundary conditions at infinity. A wide discussion on the treatment of this open boundary problem can be found

0018-9464/88/0100-0098$01.00©1988 IEEE

in [9,10,11], where it is suggested to close the problem by coupling finite element methods with boundary solution procedures.This allows us to restrict the study to a finite domain, on whose boundary an integral equation has to be satisfied. The couplings proposed present, however, two drawbacks: the resulting dynamic matrices are no longer symmetric and a careful numerical treatment of the singular kernel of the integral equation is required.

Thus we have examined the possibility of using other approaches which overcome these difficulties.

The first one is a classical coordinate transformation (inversion with respect to a sphere V_b of radius ρ_b that encloses the conducting region). Only the domain V_b is discretized, but the region R^3-V_b is included in the analysis by means of the mapping $\underline{X} = (\rho_b^2/|\underline{x}|^2)\underline{x}$. In this way Eq. (10) is modified as follows:

$$\int_{V_c} \text{grad } \Omega_k \cdot \underline{\mu} \cdot (\underline{T}-\text{grad } \Omega) d\tau + - \int_{V_b} \text{grad } \Omega_k \cdot \mu_o \cdot \text{grad } \Omega \cdot \frac{\rho_b^2}{|\underline{x}|^2} d\tau = 0, \quad \forall \Omega_k \qquad (13)$$

The second approach is a coupling between finite element methods and boundary solution procedures which yields symmetric positive definite matrices, as shown in [4] for a two-dimensional application.

If the analysis is carried out within a bounded domain V_o (which encloses all sources, conductors, inhomogeneities and nonlinearities), Eq. (10) takes the form:

$$\int_{V_o} \text{grad } \Omega_k \cdot \underline{\mu} \cdot (\underline{T}-\text{grad } \Omega) d\tau + + \int_{V_o} \Omega_k \, (\underline{\mu} \cdot \text{grad } \Omega) \cdot \hat{n} \, d\Sigma = 0, \quad \forall \Omega_k \qquad (14)$$

If V_o is taken to be the sphere V_b, then the term $\hat{n} \cdot \underline{\mu} \cdot \text{grad}\Omega = \mu_o \, \partial\Omega/\partial n$, under the constraint that div grad $\Omega = 0$ outside V_b, can be directly related to the values attained by Ω on ∂V_b. The procedure makes use of Green's functions and is described in [4]. In this way Eq. (14) is transformed into the self-adjoint form:

$$\int_{V_b} \text{grad } \Omega_k \cdot \underline{\mu} \cdot (\underline{T}-\text{grad}\Omega) d\tau - \frac{\mu_o}{\rho_b} \int_{\partial V_b} \Omega_k \, \Omega \, d\Sigma + - \frac{\mu_o}{4\pi} \int_{\partial V_b} \int_{\partial V_b} \frac{(\Omega_k-\Omega_k') \cdot (\Omega-\Omega')}{|\underline{x}-\underline{x}'|^3} d\Sigma \, d\Sigma' = 0, \; \forall \Omega_k \qquad (15)$$

RESULTS AND CONCLUSIONS

On the basis of the differential formulation described in this paper, we have developed CARDIFF, a finite element code which handles the open boundary problem of the analysis of the eddy currents induced in fully three-dimensional (magnetic) conductors.

Results and efficiency of different treatments of the regularity conditions at infinity (coordinate transformation, coupling with an integral equation on the boundary of the integration domain, and homogeneous Dirichlet or Neumann conditions at finite distance) are compared with those of CARIDDI, a finite element code based on the $\underline{T}$ integral formulation [3].

For this purpose we have analysed the eddy currents induced in a hollow conducting sphere. For this simple case, proposed at the International Electromagnetic Workshop on the comparison of computer codes (Graz, 1987), an analytical solution is available.

The hollow sphere (internal radius ρ_i = 50 mm, external radius ρ_e = 55 mm, resistivity $\eta = 2 \cdot 10^{-9}$ Ωm) is excited by a uniform sinusoidal field (B_M = 1 T, f = 50 Hz). As both codes do not work in the frequency domain, time integrations (using Crank-Nicholson scheme) have been performed until sinusoidal regimes have been reached. The linearity of the problem has allowed to solve the differential equations in terms of the (eddy) induced field alone.

In order to exploit a number of symmetries, only 1/8 of the region has been discretised. The meshes used for the calculations have been produced via MODULEF [12] and are shown in Figs. 1÷6. Twelve runs have been performed in order to compare accuracy, storage occupation and CPU time consumption.

The first one has been executed with CARIDDI, and obviously only the conducting region has been discretised (Fig. 1).

The second one has been performed with CARDIFF, applying the coordinate transformation (CT) which yields Eq. (13); the region V_b has been chosen as a sphere of radius ρ_b = 55 mm, and the mesh is shown in Fig. 2.

Two runs have been done with CARDIFF using the coupling with the boundary solution procedure (BSP) according to Eq. (15). The two cases refer to spheres of radii ρ_b = 55 mm (Fig. 2) and ρ_b = 85 mm (Fig. 3) respectively.

Finally, 2x4 runs have been performed with CARDIFF using the simple approach of imposing homogeneous Dirichlet (D) or Neumann (N) boundary conditions on the surfaces of four spheres surrounding the conducting region. The radii of these spheres are 85, 160, 300 and 600 mm respectively, and the relative meshes are shown in Figs. 3÷6.

Some numerical results concerning total eddy current, induced magnetic field at the center of the sphere, ohmic power and stored magnetic energy are reported in Tab. 1 for the different cases and compared with the analytical solution.

In Tab. 2 are given number of unknowns, size of the dynamic matrices, CPU time consumptions on a MICROVAX-II computer. The CPU times are divided into time required for the construction of the matrices and time required for the transient analysis.

As we have used the mesh suggested by the International Electromagnetic Workshop, the results show a good agreement with the analytical solution with the exception of the ohmic power. This is clearly explained by the fact that the mesh size is of the order of magnitude of the skin depth at 50 Hz.

A first comparison can be made between integral and differential methods, when nonmagnetic media are concerned. As a matter of fact it should be pointed out that the test case of the hollow sphere is particularly favorable to the integral approach, as the conducting region has the structure of a thin shell. However, the results show that the CPU time required for building the dynamic matrices is higher for the integral method, and the difference can considerably grow up when fully three-dimensional structures are considered and when symmetries of rotation are present. Nevertheless the storage occupations plays in favour of the integral procedures as well as the CPU time required for the transient analysis, which scales with the size of the dynamic matrices. It is worth noticing that in Tab. 2 the memory occupation of CARIDDI refers to a single full matrix storage, while the data reported as for CARDIFF refer to a pair of symmetric banded matrices (the optimizations of the bands have been performed by means of the algorithm of Cuthill-McKee [13]). It must be noticed, however, that the conclusions on CPU time consumptions may be modified if a parallel processor is employed.

As far as the treatment of the regularity conditions at infinity is concerned, the best results have been doubtless obtained with the formulation (15). Good results have been achieved also with the coordinate transformation; the efficiency of this procedure could be however improved with a better dis-

cretization of the mapping of the outer region.

Finally, it can be noticed that imposing homogeneous Dirichlet or Neumann conditions at finite distance attains a comparable accuracy only at high values of ρ_b. The seemingly better precision achieved by imposing Neumann boundary conditions at ρ_b = 300 mm is to be ascribed to a compensation between truncation error due to the finite mesh size and approximation error in applying boundary conditions.

REFERENCES

[1] A. Bossavit, J.C. Vérité: "A Mixed FEM-BIEM Method to Solve 3-D Eddy Current Problems", IEEE Trans. Mag., MAG-18(2), 1982, pp. 431-435.

[2] M.L. Brown: "Calculation of 3-D Eddy Currents at Power Frequencies", IEE Proc., Vol. 129, PtA, n. 1, 1982, pp. 46-53.

[3] R. Albanese, G. Rubinacci: "An Integral Formulation for 3-D Eddy Current Computation Using Nonconformal Elements", to be published.

[4] R. Albanese, J. Blum, O. De Barbieri: "On the solution of the Magnetic Flux Equation in an Infinite Domain", Europh. Conf. Abstract, 8th Europh.Conf. on Computational Physics, Eibsee (1986), Vol. 10 D, pp. 41-44.

[5] C.J. Carpenter: "Comparison of Alternative Formulations of 3-D Magnetic Field and Eddy Current Problems at Power Frequencies", IEE Proc., Vol. 124, n. 11, 1977, pp. 1026-1034.

[6] R. Albanese, R. Martone, G. Miano, G. Rubinacci: "A T Formulation for the 3-D F.E. Eddy Current Computation", IEEE Trans. Mag., MAG-21, n. 6, Nov. 1985, pp. 2299-2302.

[7] J.C. Nedelec: "Mixed Finite Elements in R³", Numerische Mathematik, 35, pp. 315-341.

[8] J.S. van Welij: "Calculation of Eddy Currents in terms of H on Hexaedra", IEEE Trans. Mag., MAG-21, N. 6, Nov. 1985, pp. 2239-2241.

[9] B.H. Mc Donald, A. Wexler: in Finite Elements in Electrical and Magnetic Field Problems, M.V.K. Chari et al., Eds. Wiley (1980), pp. 161-190.

[10] O.C. Zienkiewicz, D.W. Kelly, P. Bettes: in Energy Methods in Finite Element Analysis, R. Glowinski et al., Eds. Wiley (1979), pp. 81-107.

[11] M.V.K. Chari et al.: "Solution of Open Boundary Problems by Differential and Integral Methods", IEEE Trans. Mag., MAG-22 (5), pp. 1037-1039.

[12] M. Bernadou, P.L. George, P. Laug, M. Vidrascu: "MODULEF: a Library of Computer Procedures for Finite Element Analysis", Structural analysis systems, Ed. A. Niku-Lari, Vol. 3, Pergamon Press, 1986.

[13] E. Cuthill, J. McKee: "Reducing the Bandwidth of Sparse Symmetric Matrices", Proc. of 24th Conf. of the ACM, ACM Publ. P-69, New York (1969), pp. 157-172.

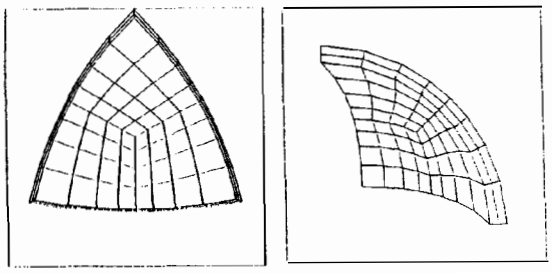

Fig. 1: Discretization of the conducting region (183 nodes, 96 elements)

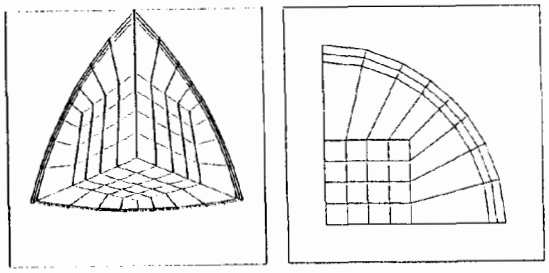

Fig. 2: Discretization of the region $\rho \leq 55$ mm (308 nodes, 208 elements)

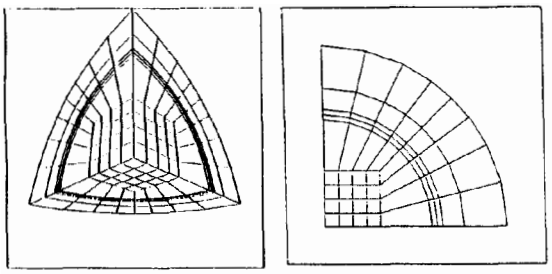

Fig. 3: Discretization of the region $\rho \leq 85$ mm (430 nodes, 304 elements)

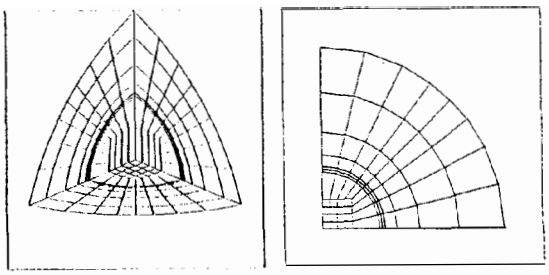

Fig. 4: Discretization of the region $\rho \leq 160$ mm (552 nodes, 400 elements)

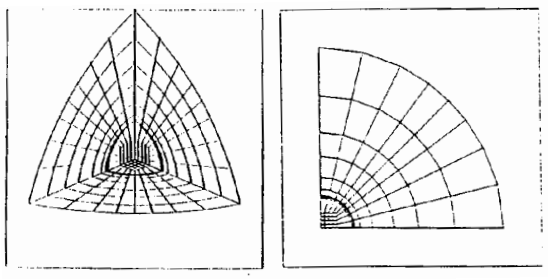

Fig. 5: Discretization of the region $\rho \leq 300$ mm (674 nodes, 496 elements)

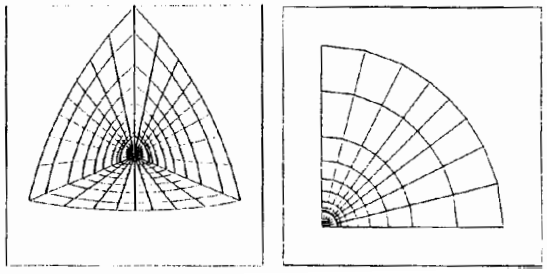

Fig. 6: Discretization of the region $\rho \leq 600$ mm (796 nodes, 592 elements)

Table 1

Results obtained using the different formulations

	Total Eddy Current $I(t) = I_o \sin(2\pi ft + \phi_I)$				Ohmic Power $P(t) = P_a + P_o \cos(4\pi ft + \phi_p)$					
	I_o(kA)	ε(%)	ϕ_I(deg)	ε(%)	P_a(kW)	ε(%)	P_o(kW)	ε(%)	ϕ_p(deg)	ε(%)
CARIDDI	131.0	0.18	183.1	-0.01	9.290	-7.66	6.027	0.24	201.5	-3.52
CARDIFF-CT	129.4	-1.05	183.0	-0.05	9.098	-9.58	6.007	-0.09	201.6	-3.48
CARDIFF-BSP (ρ_b=55mm)	130.8	0.05	183.1	-0.02	9.204	-8.52	6.078	1.09	201.6	-3.46
CARDIFF-BSP (ρ_b=85mm)	129.9	-0.65	183.1	-0.03	9.087	-9.68	6.000	-0.21	201.6	-3.49
CARDIFF-D (ρ_b=85mm)	115.7	-11.6	182.6	-0.27	7.207	-28.5	4.758	-20.9	200.7	-3.90
CARDIFF-N (ρ_b=85mm)	172.4	31.8	184.5	0.76	16.003	59.1	10.566	75.7	204.2	-2.25
CARDIFF-D (ρ_b=160mm)	127.1	-2.85	183.0	-0.08	8.691	-13.6	5.739	-4.55	201.4	-3.57
CARDIFF-N (ρ_b=160mm)	134.3	2.71	183.2	0.04	9.716	-3.43	6.415	6.69	201.9	-3.34
CARDIFF-D (ρ_b=300mm)	128.9	-1.40	183.0	-0.05	8.953	-11.0	5.911	-1.69	201.5	-3.52
CARDIFF-N (ρ_b=300mm)	130.0	-0.56	183.1	-0.03	9.105	-9.50	6.011	-0.02	201.6	-3.48
CARDIFF-D (ρ_b=600mm)	129.3	-1.16	183.0	-0.05	8.994	-10.6	5.939	-1.22	201.6	-3.51
CARDIFF-N (ρ_b=600mm)	129.4	-1.06	183.1	-0.04	9.014	-10.4	5.951	-1.02	201.6	-3.50

	Induced Magnetic Field at the Center $B(t) = B_o \sin(2\pi ft + \phi_B)$				Stored Energy of Induced Field $E(t) = E_a + E_o \cos(4\pi ft + \phi_E)$					
	B_o(T)	ε(%)	ϕ_B(deg)	ε(%)	E_a(J)	ε(%)	E_o(J)	ε(%)	ϕ_E(deg)	ε(%)
CARIDDI	1.042	0.59	182.5	0.11	187.3	-2.14	185.3	-1.61	187.1	-0.16
CARDIFF-CT	1.040	0.37	182.5	0.11	185.6	-2.99	183.6	-2.49	187.3	-0.07
CARDIFF-BSP (ρ_b=55mm)	1.040	0.39	182.5	0.11	186.7	-2.42	184.7	-1.92	187.4	-0.04
CARDIFF-BSP (ρ_b=85mm)	1.040	0.37	182.5	0.10	185.6	-3.03	183.6	-2.54	187.3	-0.07
CARDIFF-D (ρ_b=85mm)	1.036	0.02	182.2	-0.04	165.3	-13.6	163.8	-13.0	186.3	-0.59
CARDIFF-N (ρ_b=85mm)	1.051	1.52	183.2	0.52	245.7	28.4	242.2	28.6	189.7	1.20
CARDIFF-D (ρ_b=160mm)	1.039	0.29	182.4	0.07	181.5	-5.16	179.6	-4.65	187.1	-0.16
CARDIFF-N (ρ_b=160mm)	1.041	0.49	182.6	0.15	191.8	0.23	189.7	0.71	187.6	0.06
CARDIFF-D (ρ_b=300mm)	1.039	0.34	182.5	0.09	184.2	-3.75	182.2	-3.25	187.3	-0.10
CARDIFF-N (ρ_b=300mm)	1.040	0.37	182.5	0.10	185.7	-2.95	183.7	-2.45	187.3	-0.07
CARDIFF-D (ρ_b=600mm)	1.039	0.35	182.5	0.10	184.6	-3.53	182.6	-3.03	187.3	-0.09
CARDIFF-N (ρ_b=600mm)	1.039	0.35	182.5	0.10	184.8	-3.43	182.8	-2.93	187.3	-0.09

Table 2

Memory and CPU times required by the different formulations

	Number of unknowns	Memory occupation of dynamic matrices	CPU time(s) (formation of the matrices)	CPU time(s) (transient analysis: 4900 time steps)	CPU time(s) (total)
CARIDDI	152	23104	1923	1537	3460
CARDIFF-CT	707	2 x 53257	123	23205	23328
CARDIFF-BSP(ρ_b= 55 mm)	460	2 x 37591	790	13767	14557
CARDIFF-BSP(ρ_b= 85 mm)	582	2 x 46115	838	16865	17703
CARDIFF-D/N (ρ_b= 85 mm)	582	2 x 44765	144	16492	16636
CARDIFF-D/N (ρ_b= 160mm)	704	2 x 53289	196	19480	19676
CARDIFF-D/N (ρ_b= 300mm)	826	2 x 61813	270	22508	22778
CARDIFF-D/N (ρ_b=600mm)	948	2 x 70337	342	25572	25914